

The role of attractive interactions in the dynamics of molecules in liquids

X. You, L. R. Pratt

Department of Chemical and Biomolecular Engineering, Tulane University, New Orleans, LA 70118

S. W. Rick

Department of Chemistry, The University of New Orleans, New Orleans, LA 70148

(Dated: June 14, 2021)

The friction kernel (or memory function) $\gamma(t)$ characterizing single-molecule dynamics in strongly bound liquids exhibits two distinct relaxations with the longer time-scale relaxation associated with attractive intermolecular forces. This observation identifies differing roles of repulsive and attractive interaction in the motions of molecules in equilibrium liquids, and thus provides a basis for a renewed investigation of a van der Waals picture of the transport properties of liquids. This conclusion is supported by extracting $\gamma(t)$ from molecular dynamics simulation data for four common molecular liquids.

INTRODUCTION

A basic goal of the molecular theory of liquids is the clear discrimination of effects of intermolecular interactions of distinct types, *e.g.* excluded volume interactions and longer ranged attractive interactions [1, 2]. That discrimination leads to the van der Waals picture [1, 3, 4] of the equilibrium theory of classical liquids. Those ideas are clear enough to be captured in models with van der Waals *limits* that are susceptible to rigorous mathematical analysis [5]. Ultimately, the general theory of liquids is then founded on the composite van der Waals picture which also serves to characterize non-van der Waals cases, such as water, for particular scrutiny [6]. Here we obtain observations that distinguish differing roles of repulsive and attractive interaction in the dynamics of molecules in equilibrium liquids.

The analogue of the van der Waals picture of equilibrium liquids for transport properties is much less developed. That is partly because of the higher variety of transport phenomena to be addressed [7]. It is also because the mathematical van der Waals limit contributes essentially at *zeroth* order to the thermodynamics, whereas extensions of van der Waals concepts to transport parameters have shown that the leading contribution typically comes at higher order [8]. The leading contribution from attractive interactions to a self-diffusion coefficient vanishes in the van der Waals limit [9] though the equation of state changes qualitatively in the same limit.

Nevertheless, it is important accurately to characterize the contributions of realistic attractive interactions to kinetic characteristics of liquids. This has been the serious topic of previous investigations [10, 11]. One distinction of the work here from previous efforts is that we focus on a specific autocorrelation function of the random forces on a molecule in the liquid, $\gamma(t)$ defined below.

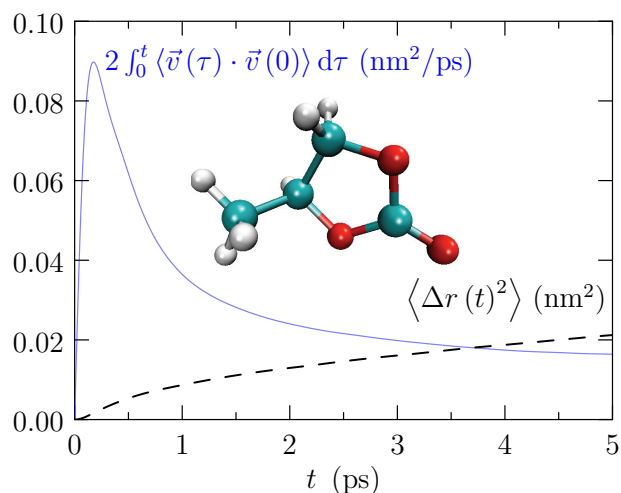


FIG. 1. Dashed curve: the mean-square-displacement of the center-of-mass of a propylene carbonate molecule in liquid PC. $D_{PC} = 4.0 \times 10^{-6} \text{ cm}^2/\text{s}$. Solid curve: time-derivative of the mean-square-displacement. The inset depicts the propylene carbonate (PC) molecule. The molecular dynamics simulation utilized the GROMACS package in the isothermal-isobaric ensemble (NPT) with periodic boundary conditions and $p = 1 \text{ atm}$. The GROMACS OPLS all-atom force field was adopted for liquid PC, and temperature $T = 300\text{K}$ maintained by Nose-Hoover thermostat. The system of $n = 1000$ PC molecules was aged for 10 ns, then a 1 ns trajectory was obtained, saving configurations every 10th 1 fs time step for analysis.

Another distinction is that we consider practical examples of solvent liquids that are strongly bound compared to the Lennard-Jones (LJ) models that have been the focus of historical work. We characterize this ‘strongly bound’ distinction by the ratio of the critical-point to the triple-point temperatures (T_c/T_t). For the LJ fluid this ratio is $T_c/T_t = 1.9$, but here we consider propylene carbonate (PC: 3.5), ethylene carbonate (EC: 2.3), acetonitrile (AN: 2.4), and water (W: 2.4). In these practical cases, attractive interactions leading to the greater bind-

ing strength are more prominent than in the historical LJ work.

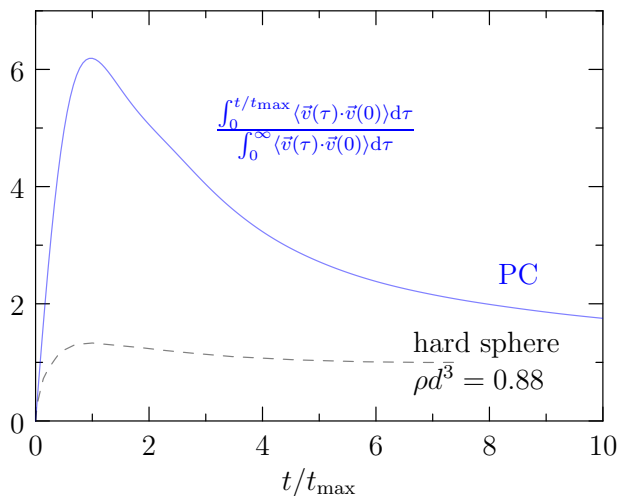


FIG. 2. Normalized time-derivative of the mean-square displacement of a molecule center-of-mass. The blue curve is redrawn from FIG. 1, with the vertical scaling so that the graph equals one (1) at large time, and the horizontal scaling so that the graph has a maximum at the time t_{\max} . The dashed curve is the result for the hard sphere fluid, redrawn from Alder, *et al.* [12]. The density, $\rho d^3 = 0.88$, is within about 5% of the hard-sphere freezing point. The maximum in these graphs occurs when $C(t)$ changes sign. The result for the realistic PC fluid is qualitatively different from the result for the hard sphere case.

Primitive results that motivate our observations are shown in FIGs. 1 and 2. The mean-square-displacement $\langle \Delta r(t)^2 \rangle$ of the center-of-mass of a PC molecule in liquid PC (FIG. 1) achieves growth that is linear-in-time only after tens of collision-times. The time-derivative of $\langle \Delta r(t)^2 \rangle$ displays a prominent maximum that can be taken as a rough marker for a collision time. After that, the derivative decreases by more than a factor of ten, reflecting the integrated strength of a negative tail of the velocity autocorrelation function,

$$C(t) = \langle \vec{v}(t) \cdot \vec{v}(0) \rangle / \langle v^2 \rangle . \quad (1)$$

That negative tail is qualitatively different from the case of the hard-sphere fluid at high densities (FIG. 2) [12]. More recent studies of atomic fluids with purely repulsive inter-atomic forces show that negative tails in the velocity autocorrelation functions are slight [13, 14]. The result for the realistic PC fluid is qualitatively different from the atomic repulsive force case.

METHODS

We focus on the friction kernel (memory function), $\gamma(t)$ defined by

$$M \frac{dC(t)}{dt} = - \int_0^t \gamma(t - \tau) C(\tau) d\tau , \quad (2)$$

where M is the mass of the molecule. $\gamma(t)$ can be considered the autocorrelation function for the *random* forces on a molecule [15]. The textbook method for extracting $\gamma(t)$ utilizes standard Laplace transforms. But inverting the Laplace transform is non-trivial and we have found the well-known Stehfest algorithm [16] to be problematic. Berne and Harp [17] developed a finite-difference-in-time procedure for extracting $\gamma(t)$ from Eq. (2). That procedure is satisfactory but sensitive to time resolution in the numerical $C(t)$ that is used as input here. Another alternative expresses the Laplace transform as Fourier integrals, utilizing specifically the transforms

$$\hat{C}'(\omega) = \int_0^\infty C(t) \cos(\omega t) dt , \quad (3a)$$

$$\hat{C}''(\omega) = \int_0^\infty C(t) \sin(\omega t) dt . \quad (3b)$$

Then

$$\int_0^\infty \gamma(t) \cos(\omega t) dt = \frac{M \hat{C}'(\omega)}{\hat{C}'(\omega)^2 + \hat{C}''(\omega)^2} . \quad (4)$$

Taking $\gamma(t)$ to be even time, the cosine transform is straightforwardly inverted. $\Omega^2 = \langle F^2 \rangle / 3Mk_B T$, with $F = |\vec{F}|$ the force on the molecule, provides the normalization $\gamma(0) = M\Omega^2$.

RESULTS AND DISCUSSION

The two numerical methods for extracting $\gamma(r)$ from $C(t)$ agree well (FIG. 3). $\gamma(t)/M\Omega^2$ for four strongly bound liquids are qualitatively similar to each other and show two distinct relaxations. The historical LJ results [10, 11] are consistent with this, though the two relaxation behaviors are distinct for the LJ fluid only at the lowest liquid temperatures [11]. We suggest that the slowest-time relaxation derives from molecularly long-ranged interactions, while the fastest-time relaxation is associated with collisional events and short-ranged interactions. This discrimination of long-ranged and short-ranged interaction effects was expressed by Wolynes [18] long-ago in the context of ion mobilities in solution. Here mobilities of non-ionic species are considered, though similar behavior has been identified in just the same way for organic ions in solution [19]. The results for liquid PC at several higher temperatures (FIG. 4) show that the amplitude of this longer-time-scale decay decreases with increasing T , as expected.

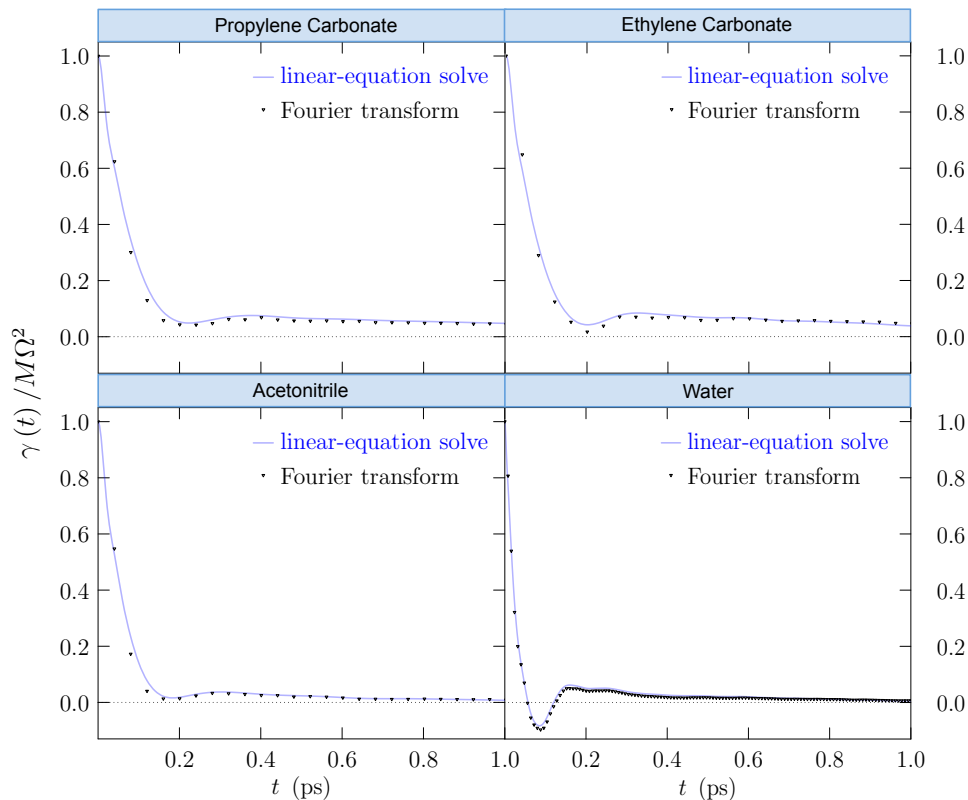


FIG. 3. $\gamma(t)$, the friction kernel (or memory function). All the simulations used the GROMACS package and periodic boundary conditions, with $p = 1$ atm in the isothermal-isobaric ensemble. PC calculations were specified with FIG. 1. For the acetonitrile, simulation the force-field of Nikitin and Lyubartsev [20] was assumed. For ethylene carbonate, we used the GAFF force field [21], a system size of 215 molecules at $T = 313$ K. For the water simulation, the TIP4P-EW model [22] was used, and the trajectory was saved every 1 fs.

By comparison, Dang and Annapureddy [24, 25] evaluated $\gamma(t)$ for Dang-Chang-model water [26] in a different setting, and they obtained the distinct bi-relaxation observed here. In that alternative setting, the separation between a water oxygen atom and a near-neighbor ion was constrained at a barrier value and $t > 0$ negative values of $\gamma(t)$ (FIG. 3) were not observed [24, 25].

The longer-time scale decay of $\gamma(t)$ (FIG. 3) is less prominent for the liquid water case than for the other cases. We investigated this further by eliminating the partial charges associated with the pair-molecule interactions, leaving LJ 6-12 interactions (FIGs. 5 and 6). That underlying LJ case is strongly super-critical. Furthermore, with the implied high-density of the underlying LJ system, the continuous-repulsive-force ($1/r^{12}$) case in

not similar to the result from the previous study of Heyes *et al.* [14]; we observe a distinct recoil feature at this density.

CONCLUSIONS

For strongly bound liquids, the friction kernel (or memory function) $\gamma(t)$ (Eq. (2)) exhibits two distinct relaxations with the longer time-scale relaxation associated with attractive intermolecular forces.

ACKNOWLEDGEMENT

This work was supported by the National Science Foundation under the NSF EPSCoR Cooperative Agreement No. EPS-1003897, with additional support from the Louisiana Board of Regents.

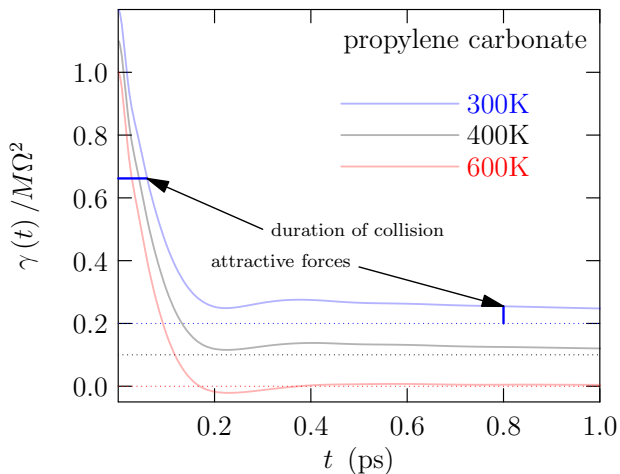


FIG. 4. Autocorrelation function for the random forces on the center-of-mass of a propylene carbonate molecule as a function of temperature at constant pressure, $p = 1$ atm. The longer time-scale relaxation becomes less prominent at higher T .

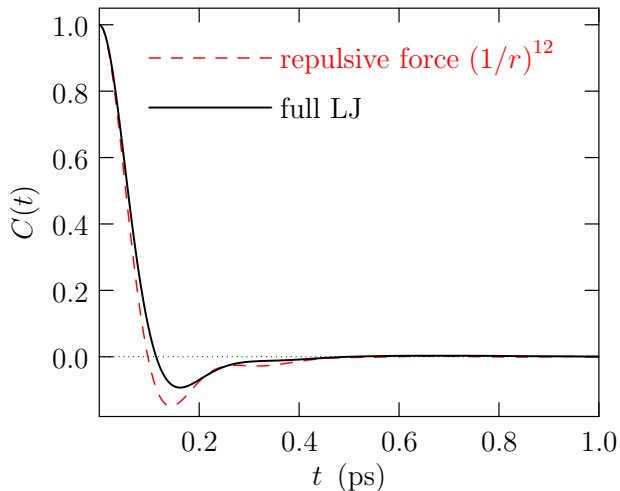


FIG. 5. Velocity autocorrelation function for the LJ 6-12 fluid and the corresponding result when the $1/r^6$ contribution to the pair potential energy is dropped. The LJ thermodynamic state point is $\rho\sigma^3 = 1.06$, and $k_B T/\epsilon = 3.66 \approx 2.8T_c$ [23]. For the $1/r^{12}$ case, this density is slightly higher than a high density cases studied by Heyes *et al.* [14], (effective packing fraction $\xi_{HS} \approx 0.466$ compared to 0.45).

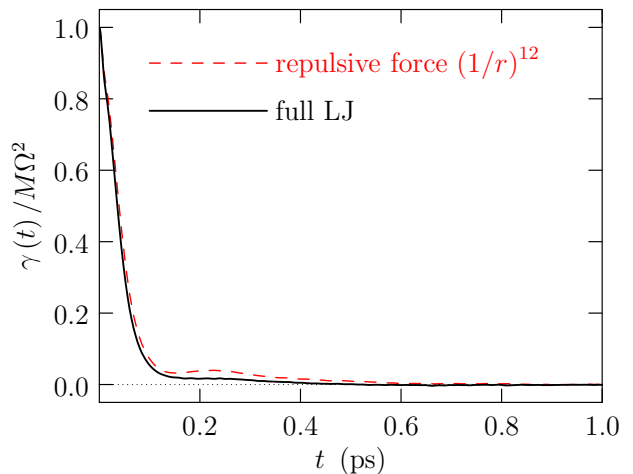


FIG. 6. For the LJ system of FIG. 5. The second, longer-time-scale relaxation is not evident at this thermodynamic state which is a high density state, super-critical for the LJ liquid. Thus, the longer-time-scale relaxation of Fig. 3 for water, is due to the electrostatic interactions that contribute largely to the cohesive binding of liquid water.

[1] B. Widom, *Science* **157**, 375 (1967).
 [2] H. C. Andersen, D. Chandler, and J. D. Weeks, *Adv. Chem. Phys.* **34**, 105 (1976).
 [3] J. A. Barker and D. Henderson, *Rev. Mod. Phys.* **48**, 587 (1976).
 [4] D. Chandler, J. D. Weeks, and H. C. Andersen, *Science* **220**, 787 (1983).
 [5] J. L. Lebowitz and E. M. Waisman, *Phys. Today*, 24 (1980).

[6] J. Shah, D. Asthagiri, L. Pratt, and M. Paulaitis, *J. Chem. Phys.* **127**, 144508 (1 (2007)).
 [7] R. Zwanzig, *Ann. Rev. Phys. Chem.* **16**, 67 (1965).
 [8] P. Resibois, J. Piasecki, and Y. Pomeau, *Phys. Rev. Letts.* **28**, 882 (1972).
 [9] M. Seghers, P. Resibois, and Y. Pomeau, *Phys. Letts.* **53A**, 353 (1975).
 [10] L. Verlet, *Phys. Rev.* **159**, 98 (1967).
 [11] J. Kushick and B. J. Berne, *J. Chem. Phys.* **59**, 3732 (1973).
 [12] B. J. Alder, D. M. Gass, and T. E. Wainwright, *J. Chem. Phys.* **53**, 3813 (1970).
 [13] D. M. Heyes and J. G. Powles, *Mol. Phys.* **95**, 259 (1998).
 [14] D. M. Heyes, J. G. Powles, and G. Rickayzen, *Mol. Phys.* **100**, 595 (2002).
 [15] D. Forster, *Hydrodynamic fluctuations, broken symmetry, and correlation functions*, Frontiers in Physics, Vol. 47 (WA Benjamin, Inc., Reading, Mass., 1975).
 [16] H. Stehfest, *Comm. ACM* **13**, 47 (1970).
 [17] B. J. Berne and G. Harp, *Adv. Chem. Phys.* **17**, 63 (1970).
 [18] P. G. Wolynes, *J. Chem. Phys.* **68**, 473 (1978).
 [19] P. Zhu, L. Pratt, and K. Papadopoulos, *J. Chem. Phys.* **137**, 174501 (2012).
 [20] A. M. Nikitin and A. P. Lyubartsev, *J. Comp. Chem.* **28**, 2020 (2007).
 [21] J. M. Wang, R. M. Wolf, J. W. Caldwell, P. A. Kollman, and D. A. Case, *J. Comp. Chem.* **25**, 1157 (2004).
 [22] H. W. Horn, W. C. Swope, J. W. Pitera, J. D. Madura, T. J. Dick, G. L. Hura, and T. Head-Gordon, *J. Chem. Phys.* **120**, 9665 (2004).
 [23] B. Smit, *J. Chem. Phys.* **96**, 8639 (1992).
 [24] L. X. Dang and H. V. R. Annapureddy, *J. Chem. Phys.* **139**, 084506 (2013).
 [25] H. V. R. Annapureddy and L. X. Dang, *J. Phys. Chem. B* **118**, 8917 (2014).
 [26] L. X. Dang and T.-M. Chang, *J. Chem. Phys.* **106**, 8149 (1997).